Methanol desorption in poly(methyl methacrylate) with stress distributions

Donyau Chiang
Instrument Technology Research Center, National Applied Research Laboratories, Hsinchu 300, Taiwan

Fuqian Yang
Department of Chemical and Materials Engineering, University of Kentucky, Lexington, Kentucky 40506, USA

Chi Wei Liu, Kuo-Chen Ho, and Sanboh Lee[a)]
Department of Materials Science and Engineering, National Tsing Hua University, Hsinchu 300, Taiwan

(Received 15 May 2014; accepted 29 July 2014)

Understanding solvent transport in polymers is of practical importance for the applications of polymers in the fields of food packaging, biomedical bandages, materials engineering, etc. We studied one-side desorption in poly(methyl methacrylate) (PMMA). Experimental results showed that methanol desorption in PMMA depended on temperature and the initial distribution of concentration. The diffusion coefficient in PMMA and the evaporation rate of methanol across the PMMA surface followed the Arrhenius relation. The activation energies for the diffusion and the evaporation of methanol are 18.3, 42.6 and 8.6, 18.3 kJ/mol for the specimens with the ratio of initial mass to the equilibrium saturated absorbed mass, M_i/M_∞, being 14.6% and 35.3%, respectively. The partial molal volume increased with the increase of the desorption temperature for $M_i/M_\infty = 14.6\%$, while it had an opposite trend for $M_i/M_\infty = 35.5\%$. The chemical stresses developed in PMMA during the desorption were also studied.

I. INTRODUCTION

Alfrey et al.[1] proposed that the transport behavior of solvents in polymers can be categorized as Case I, Case II and anomalous transport. The Case I transport is dominated by Fickian diffusion and the Case II transport is controlled by stress relaxation of polymer chains. Anomalous transport occurs when the effect of solvent penetration is comparable to the effect of stress relaxation. Chen and Edin[2] studied the Case I diffusion of bisphenol-A in polycarbonate. Crank[3] solved various diffusion problems for different geometries and boundary conditions. Thomas and Windle[4] attributed the Case II transport to the advancement of a sharp interface at a constant velocity, which separates an inner glassy core from an outer swollen layer. Friedman and Rossi[5] identified the transition surface between the glassy state and the rubber state for the Case II kinetics. Hui and Wu[6,7] studied the transient swelling and the steady-state front motion in the Case II transport. Kwei et al.[8] were the first group to propose an equation for describing the anomalous transport of solvent in polymers. Their solution was only valid for semi-infinite materials. Harmon et al.[9,10] modified Kwei's equation and applied it to specimens of finite sizes; they also solved and extended the transport kinetics to various solvent–polymer systems.[11–14] All the above studies had been concentrated on the mass uptake in polymeric materials where the glassy core and the outer rubber-state material are separated by a sharp interface.

Understanding the desorption of solvent in polymers is of great importance from both the fundamental and practical points of view. For example, polymer films of moderate mechanical strength and suitable permeability are needed to limit the residual amount of specific gases in food packaging,[15] medical bandages,[16] electronic packaging,[17] etc. The film characteristics are strongly dependent on the drying and cooling processes, and the solvent transport plays an important role in the drying process. It has been proposed that factorial design needs to analyze the sorption/desorption mechanisms.[18] Yang et al.[19] reported the desorption and pervaporation of zeolite-filled poly(dimethylsiloxane) membranes. Saby-Dubreuil et al.[20] examined the effect of solvent desorption on the glass transition of the

[a)]Address all correspondence to this author.
e-mail: sblee@mx.nthu.edu.tw
DOI: 10.1557/jmr.2014.232

 © Materials Research Society 2014

https://doi.org/10.1557/jmr.2014.232 Published online by Cambridge University Press

statistical MMA/nBMA copolymer, and found a strong coupling between drying dynamics and stress relaxation. Gommes et al.[21] measured the isothermal methanol desorption in silicon gels. None of these studies have considered the anomalous transport followed by desorption, the effect of one-side desorption on desorption behavior, and the stress relaxation in polymer slabs. This has prompted us to study the methanol desorption in poly(methyl methacrylate) (PMMA).

II. THEORY

A. Absorption

Harmon et al.[9] proposed a model of solvent uptake in polymers that accounts for the Case I, Case II, and anomalous transport. Consider a PMMA slab with a thickness of 2ℓ and the planar area being much larger than the lateral area. The solvent-free slab is immersed in a methanol bath. At the interfaces between the slab and methanol ($x = 0$ and $x = 2\ell$), the solvent concentration is maintained at a constant, C_0. The diffusion flux is assumed as a linear combination of the Case I and Case II transports, and methanol always diffuses toward the center of the slab. The concentration distribution of methanol at any instant time t during the uptake can be found as[9]

$$\frac{C_A(x,t)}{C_0} = 1 - 2e^{(v/2D)x}\sum_{n=1}^{\infty}\frac{\lambda_n\ \sin(\lambda_n x/\ell)}{\beta_n^2[1+(2D/v\ell)\cos^2\lambda_n]}e^{-\beta_n^2 Dt/\ell^2} \quad \text{for } 0 < x < l \quad , \tag{1}$$

and

$$\frac{C_A(x,t)}{C_0} = 1 - 2e^{(v/2D)(2\ell-x)}\sum_{n=1}^{\infty}\frac{\lambda_n\ \sin[\lambda_n(2\ell-x)/\ell]}{\beta_n^2[1+(2D/v\ell)\cos^2\lambda_n]}e^{-\beta_n^2 Dt/\ell^2} \quad \text{for } 0 < x < 2\ell \quad , \tag{2}$$

with

$$\lambda_n = \frac{-v\ell}{2D}\tan\lambda_n \text{ and } \beta_n^2 = \frac{v^2\ell^2}{4D^2} + \lambda_n^2 \quad . \tag{3}$$

Here, D and v are the diffusion coefficient and the velocity for the Case I and Case II transport during the methanol absorption, respectively, and λ_n ($n = 1, 2, \ldots$) is the positive root of the first equation in Eq. (3).

Integrating Eqs. (1) and (2), we obtain the amount of methanol, M, absorbed in the PMMA slab over an immersion time t as

$$\frac{M}{M_\infty} = 1 - 2\sum_{n=1}^{\infty}\frac{\lambda_n^2\left(1-2\cos\lambda_n e^{v\ell/2D}\right)}{\beta_n^4[1+(2D/v\ell)\cos^2\lambda_n]}e^{-\beta_n^2 Dt/\ell^2} \quad , \tag{4}$$

where $M_\infty (= 2\ell C_0)$ is the equilibrium amount of methanol per unit area absorbed in the slab as the immersion time approaches infinity.

B. Desorption

After an immersion period t_a, the absorption process is terminated and the slab is removed from the methanol bath. Desorption takes place immediately. In contrast to the conventional approach of desorption through both surfaces, one surface of the slab at $x = 0$ is sealed from which no solvent can evaporate out, and the other surface at $x = 2\ell$ is exposed to the ambient environment. Thus, the initial concentration profile at the onset of desorption can be described by Eqs. (1) and (2) provided that the parameter t is replaced by t_a. It is rational to assume that the desorption process completely follows Fickian diffusion (i.e., Case I transport), since the stresses in the polymer slab have been totally relaxed during the absorption. The equation of mass transfer in the specimen of thickness 2ℓ for the one-side desorption is

$$\frac{\partial C}{\partial t} = D_1\frac{\partial^2 C}{\partial x^2} \text{ for } 0 < x < 2\ell \quad . \tag{5}$$

The boundary conditions are

$$\left.\frac{\partial C}{\partial x}\right|_{x=0} = 0 \quad , \tag{6}$$

$$\left.\frac{\partial C}{\partial x}\right|_{x=2\ell} = -h\left(C|_{x=2\ell} - C_e\right) \quad . \tag{7}$$

The initial conditions are given in Eqs. (1) and (2). Here, h is a constant, equal to the ratio of α to D_1, with α being the evaporation rate of the solvent across the surface. C_e is the equilibrium concentration of the solvent in the air environment, and its value at ambient temperature is determined from the experiment, and D_1 is the diffusion coefficient during desorption. Equation (7) represents the mass balance determined by the diffusion flux at the interface inside the slab and the evaporation rate per unit area at the interface to the air environment. The evaporation rate is only controlled by the temperature and the equilibrium concentration of the solvent in the air environment if there is no air flow.

The concentration distribution of the solvent in the slab as a function of time during the desorption is solved as

$$\frac{C}{C_0} = \frac{C_e}{C_0} + \sum_{m=0}^{\infty}A_m\ \cos(\gamma_m\, x/2\ell)e^{-\gamma_m^2 D_1 t/4\ell^2} \quad , \tag{8}$$

with $\gamma_m = 2h\ell\cot\gamma_m$,

https://doi.org/10.1557/jmr.2014.232 Published online by Cambridge University Press

$$A_m = \left[\left(1 - \frac{C_e}{C_0}\right) 2\ell \frac{\sin\gamma_m}{\gamma_m} - 2\sum_{n=1}^{\infty} \frac{\lambda_n e^{-\beta_n^2 D t_a/\ell^2} K_{mn}}{\beta_n^2 (1 + (2D/v\ell)\cos^2\lambda_n)}\right] \left(\ell + \frac{\sin^2\gamma_m}{2h}\right)^{-1} \quad ,$$

and

$$K_{mn} = \frac{-4\ell\lambda_n\left\{\left(\gamma_m^2 - 4\beta_n^2\right)(1+\cos\gamma_m) + \left(4h\ell^2 v/D\right)\cos\gamma_m + 16e^{v\ell/2D}\beta_n^2\cos\lambda_n\cos(\gamma_m/2)\right\}}{\gamma_m^4 - 8\gamma_m^2\left(\lambda_n^2 - \ell^2 v^2/4D^2\right) + 16\beta_n^4} \quad .$$

The residual amount of solvent, M_t, inside the slab during the desorption can be calculated from Eq. (8) as

$$\frac{M_t}{M_i} = \frac{C_e}{C_0} + \sum_{m=0}^{\infty} A_m \frac{\sin\gamma_m}{\gamma_m} e^{-\gamma_m^2 D_1 t/4\ell^2} \quad , \qquad (9)$$

where M_i is the total mass in the slab at the onset of the desorption and is equal to the residual mass left after the immersion time t_a in the absorption process.

C. Stress evolution in the slab during the desorption

A polymer slab expands when a solvent diffuses into the slab. The expansion proceeds with a defined pattern as stresses build up due to the solvent diffusion.[9] The stress evolution resulting from the diffusion resembles that from the temperature gradient and can be calculated by replacing the coefficient of thermal expansion and temperature with one third the value of the partial molal volume and concentration of the solvent, respectively.

Assume that the slab expands freely in the x-direction with confinement in y- and z-directions during the diffusion. In the slab, the diffusion-induced strains are $\varepsilon_y = \varepsilon_z = -\bar{V}C/3$, and the stress is $\sigma_x = 0$, in which $\overline{V}$ is the partial molal volume of the solvent in units of cm^3/mol and C is the concentration in mol/cm^3. According to the theory of linear elasticity, there is

$$\varepsilon_x = \frac{1}{E}\left[\sigma_x - \upsilon\left(\sigma_y + \sigma_z\right)\right] \quad , \qquad (10)$$

$$\varepsilon_y = \frac{1}{E}\left[\sigma_y - \upsilon\left(\sigma_x + \sigma_z\right)\right] \quad , \qquad (11)$$

$$\varepsilon_z = \frac{1}{E}\left[\sigma_z - \upsilon\left(\sigma_x + \sigma_y\right)\right] \quad . \qquad (12)$$

Substituting the diffusion-induced strains and $\sigma_x = 0$ into Eqs. (10)–(12), one obtains

$$\sigma_y = \sigma_z = -\frac{\overline{V}CE}{3(1-\upsilon)} \quad , \qquad (13)$$

where E and υ are Young's modulus and Poisson's ratio, respectively.

To calculate the diffusion-induced stresses, i.e., chemical stresses, in the slab free from any external constraints, the stresses produced in the slab must be counterbalanced by the force at the slab ends, F, as calculated below,

$$F = \frac{A}{2\ell}\int_0^{2\ell} \frac{\overline{V}CE}{3(1-\upsilon)}\,dx \quad , \qquad (14)$$

where A is the surface area of the specimen. Assume that the end effect is negligible and the force produces uniform stress in the slab at the distance far away from the slab ends. The tensile stress, σ_f, due to the force F is

$$\sigma_f = \frac{1}{2\ell}\int_0^{2\ell} \frac{\overline{V}CE}{3(1-\upsilon)}\,dx \quad . \qquad (15)$$

In addition to the tensile stress, a bending moment, M_b, is also introduced and calculated as

$$M_b = \int_0^{2\ell} \frac{\overline{V}CEA(x-\ell)}{3(1-\upsilon)}\,dx \quad . \qquad (16)$$

The bending stress, σ_b, in the slab can be calculated from the radius of curvature R as

$$\sigma_b = -\frac{E(x-\ell)}{R} \quad . \qquad (17)$$

According to the equilibrium condition that the resultant bending moment is zero, one has

$$-\int_0^{2\ell} \frac{EA(x-\ell)^2}{R}\,dx - \int_0^{2\ell} \frac{\overline{V}CEA(x-\ell)}{3(1-\upsilon)}\,dx = 0 \quad , \qquad (18)$$

which gives

$$-\frac{E}{R} = \frac{3}{2\ell^3}\int_0^{2\ell} \frac{\overline{V}CE(x-\ell)}{3(1-\upsilon)}\,dx \quad , \qquad (19)$$

and

https://doi.org/10.1557/jmr.2014.232 Published online by Cambridge University Press

$$\sigma_b = \frac{3(x-\ell)}{2\ell^3}\int_0^{2\ell}\frac{\overline{V}CE(x-\ell)}{3(1-\upsilon)}dx \quad . \tag{20}$$

From Eqs. (13), (15), and (19), the chemical stresses developed in the slab are

$$\sigma_y = \sigma_z = \frac{\overline{V}E}{3(1-\upsilon)}\left\{-C + \frac{1}{2\ell}\int_0^{2\ell} C dx + \frac{3(x-\ell)}{2\ell^3}\int_0^{2\ell} C(x-\ell)dx\right\} \quad . \tag{21}$$

Using Eq. (21), the chemical stresses in the slab can be easily calculated if the concentration profile and the partial molal volume are obtained.

D. Measurement of the partial molal volume

The partial molal volume ($\overline{V}$) of a solvent in a polymer can be determined from the measurement of the thickness change of a polymer slab. The constitutive relationships describing the diffusion-induced deformation are[22,23]

$$\varepsilon_x = \frac{1}{E}\left[\sigma_x - \upsilon(\sigma_y + \sigma_z)\right] + \frac{\overline{V}C}{3} \quad , \tag{22}$$

$$\varepsilon_y = \frac{1}{E}\left[\sigma_y - \upsilon(\sigma_x + \sigma_z)\right] + \frac{\overline{V}C}{3} \quad , \tag{23}$$

$$\varepsilon_z = \frac{1}{E}\left[\sigma_z - \upsilon(\sigma_x + \sigma_y)\right] + \frac{\overline{V}C}{3} \quad . \tag{24}$$

Substituting Eq. (21) and $\sigma_x = 0$ into Eq. (22), one obtains the diffusion-induced strain in the x-direction of the slab as

$$\varepsilon_x = \frac{\overline{V}C}{3} - \frac{2\upsilon\overline{V}}{3(1-\upsilon)}\left\{-C + \frac{1}{2\ell}\int_0^{2\ell} C dx + \frac{3(x-\ell)}{2\ell^3}\int_0^{2\ell} C(x-\ell)dx\right\} \quad . \tag{25}$$

Integrating Eq. (25) yields the thickness change of the slab, ΔL, as

$$\Delta L = \int_0^{2\ell}\varepsilon_x dx = \frac{\overline{V}}{3}\int_0^{2\ell} C dx \quad , \tag{26}$$

which can be used to determine the partial molal volume of the solvent in the polymer from the measurements of the thickness change.

III. EXPERIMENTAL DETAILS

A Lucite L-type cast acrylic PMMA sheet with a thickness of 1.03 mm was obtained from Du Pont, Wilmington, Delaware. Specimens of 20 × 6.05 × 1.03 mm^3 were cut from this sheet. The specimens were ground with emery papers of 600, 800, and 1200 grit, and were polished with 1 and 0.05 μm alumina slurries. All specimens were annealed in air for 24 h at 95 °C and furnace-cooled to ambient temperature.

Spectrograde methanol was obtained from ALPS Chem Co., Hsinchu, Taiwan. The PMMA specimens and a beaker filled with methanol were preheated individually to a temperature of 60 °C and maintained at that temperature to reach thermal equilibrium for the absorption experiments. Then, the PMMA specimens were immersed in methanol with the beaker being in a thermostatic water bath. The temperature of the water bath was maintained at 60 °C. The immersion times for two-side absorption of the slab specimens in the methanol bath were 5.07 min and 22.12 min, and the corresponding ratios of the invaded mass to the equilibrium absorbed mass, M_i/M_∞, were 14.6% and 35.3%, respectively. Note that M_∞ is 0.0742 g. The diffusivity coefficient, D, and the velocity, v, of methanol in PMMA at 60 °C were found to be 1.1 × 10^{-7} cm^2/s and 6.1 × 10^{-6} cm/s, respectively.

Immediately following the adsorption experiment, the specimens were quickly removed from the methanol bath. Both outer surfaces were blotted quickly and one surface was sealed with adhesive tape to prevent the methanol desorption from that surface. This step prevented the residual solvent and other defects on the outer surfaces from affecting desorption due to surface evaporation, because the surface evaporation is strongly dependent on the surface conditions.[24] The specimens were then suspended in an open glass tube immersed in a thermostatic water bath at different temperatures. The temperatures of the water bath were 25, 35, 45, and 55 °C for controlling the desorption rate. The weight and thickness of the specimens were measured regularly using an Ohaus analytical plus digital balance and a micrometer with a precision of 10 μm. After finishing each individual measurement, the one-side sealed specimens were immediately placed back in the glass tube to maintain the temperature and environment for the desorption experiments. Further measurements were performed until no change in the specimen weight was observed. The transverse dimensions of the specimens during the desorption were determined by stamping the transverse surface of the specimens on a graph paper, from which one can calculate the partial molal volume of methanol in PMMA from the thickness change.

IV. RESULTS AND DISCUSSION

Figure 1 shows the temporal variation of the residual mass, M_t, of the desorption PMMA specimens for the absorption times of 5.07 and 22.12 min, respectively, at several temperatures lower than the absorption temperature of 60 °C. The values of M_i/M_∞ for the specimens with the absorption times of 5.07 and 22.12 min were 14.6% and 35.3%, respectively, M_∞ is the saturated amount of methanol absorption. Note that the solid lines are obtained using Eq. (9) and the symbols represent

https://doi.org/10.1557/jmr.2014.232 Published online by Cambridge University Press

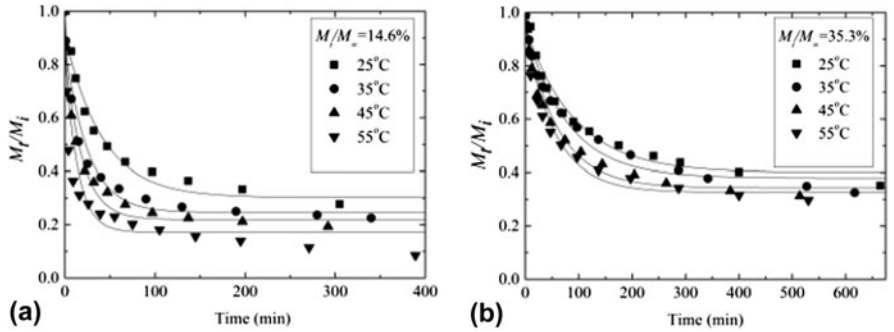


FIG. 1. Variation of the residual mass, M_t, with time for the one-side desorption of methanol in the PMMA slabs at four temperatures; (a) the absorption time is 5.07 min (M_i/M_∞ = 14.6%) and (b) the absorption time is 22.12 min (M_i/M_∞ = 35.3%).

experimental data. The amount of M_i is equal to the M value determined in Eq. (4) with t being replaced by t_a, the total immersion time. Thus, M_i represents the final mass present in the specimens after the absorption that is the amount of the initial solvent in the specimens for the desorption. The values of M_t/M_i decrease with the increase of time due to the solvent evaporation from the specimen. The decrease is significant within the times of 100 and 200 min for M_i/M_∞ = 14.6% and 35.3%, respectively, and the decrease rate of M_t/M_i gradually decreases with the increase of time afterward. For a given desorption time, the value of M_t/M_i decreases with the increase of the desorption temperature, suggesting the effect of temperature on the desorption behavior. The larger the difference between the desorption temperature and the absorption temperature, the smaller the M_t/M_i value is for the same desorption time.

Equation (9) is used to fit the experimental data in Fig. 1, and the fitting parameters are listed in Table I. Equation (9) fits the experimental results better for the initial period than the later period. This trend might result from the effect of transverse desorption and the deviation of the concentration distribution from the theoretical values due to multiple weighting operations that frequently take samples in and out of the glass tube.

Figure 2 shows the variation of D_1 and α with temperature. Both D_1 and α increase with the increase of the desorption temperature. Straight lines are drawn between the logarithm of D_1 and $1/T$ and between the logarithm of α versus $1/T$, suggesting that the temperature dependence of the diffusion and evaporation processes follows the Arrhenius relationship. The activation energies for the diffusion process in the desorption and the evaporation rate of the solvent across the surface are 18.3, 42.6 and 8.6, 18.3 kJ/mol for the specimens with the ratio of M_i/M_∞ being 14.6% and 35.3%, respectively. The rate processes are dependent on the concentration of the solvent in the PMMA specimens at the onset of the desorption, which is likely associated with the concentration dependence of the diffusion coefficient of methanol in PMMA.

TABLE I. List of the fitting parameters: diffusion coefficient, D_1; ratio of the equilibrium concentration to the saturated concentration, C_e/C_0; the evaporation rate, α; and constant, h, for the one-side desorption of methanol in the PMMA slabs with M_i/M_∞ = 0.146 and 0.353.

M_i/M_∞	T (°C)	D_1 (10^{-4} cm^2 s^{-1})	α (10^{-3} cm s^{-1})	h (cm^{-1})	C_e/C_0
0.146	55	7.05	32.4	45.95	0.025
	45	5.55	21.3	38.45	0.032
	35	4.68	13.5	28.85	0.036
	25	3.52	6.60	18.75	0.044
0.353	55	2.26	5.50	24.35	0.115
	45	2.11	4.76	22.55	0.121
	35	1.79	3.55	19.85	0.134
	25	1.68	2.86	17.05	0.137

Figure 3 shows the numerical results of the distribution of the solvent concentration in the polymer specimens with the one-side desorption at 25 °C for M_i/M_∞ being 14.6% and 35.3%. The distribution of the solvent concentration at the onset of the desorption was calculated from Eqs. (1) and (2). The parameter, $\ell v/D$, used in Fig. 3 for the absorption process was 2.85, in which ℓ, v, and D were 0.0515 cm, 6.1×10^{-6} cm/s, and 1.1×10^{-7} cm^2/s, respectively. At the onset of desorption, the solvent concentration distribution was symmetric about the central plane of the specimen, as expected, from the isotropic feature of the solvent absorption on both surfaces. During desorption, the solvent distribution became asymmetric due to the confinement to the desorption of one surface.

For M_i/M_∞ being 14.6%, the absorption time was 5.07 min which was not long enough for the solvent to diffuse into the central region of the PMMA slabs. There was continuous diffusion of the solvent toward the slab center, which was driven by the gradient of the solvent concentration during the desorption. For M_i/M_∞ being 35.3%, the absorption time was more than 22.12 min and the solvent occupied the center of the PMMA slabs. As shown in Fig. 2, one can conclude that the distribution of the solvent concentration at the onset of desorption plays an important role in determining the desorption rate.

For the one-side desorption, the solvent can only diffuse out of the polymer from the surface at $x = 2\ell$.

https://doi.org/10.1557/jmr.2014.232 Published online by Cambridge University Press

The residual amount of the solvent in the polymer decreases with increasing desorption time. The solvent concentration at $x = 2\ell$ is always less than that at $x = 0$, where the concentration gradient is zero. The values of C_e/C_0 are found to be 0.044 and 0.137 for M_0/M_∞ being 14.6% and 35.3% at 25 °C, respectively, as desorption time approaches infinity.

The thickness change of the PMMA slabs during the one-side desorption as a function of desorption time is depicted in Fig. 4 for M_i/M_∞ being 14.6% and 35.3% at different temperatures where the solid lines are obtained using Eq. (26) and the symbols represent experimental data. The thickness of the polymer slabs decreased with increasing desorption time, as expected, and eventually became constant at the final state. The constant thickness at the final state is a function of the desorption temperature. For the same desorption time, the slab thickness decreased with the increase of the desorption temperature. High temperature accelerates the evaporation of the solvent from the surface of the PMMA slabs, resulting in the fast decrease in the slab thickness.

Using Eq. (26), the partial molal volumes of 78, 85, 94, and 94 cm^3/mol are obtained for M_i/M_∞ being 14.6% and the partial molal volumes of 90, 85, 73, and 70 cm^3/mol are obtained for M_i/M_∞ being 35.5% at the desorption temperatures of 25, 35, 45, and 55 °C, respectively. The partial molal volume increases with the increase of desorption temperature for the PMMA specimens of

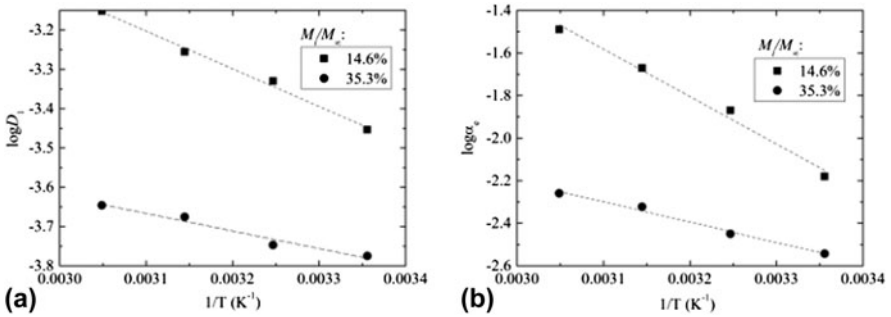


FIG. 2. Temperature dependences of (a) the diffusivity, D_1, and (b) the evaporation rate, α.

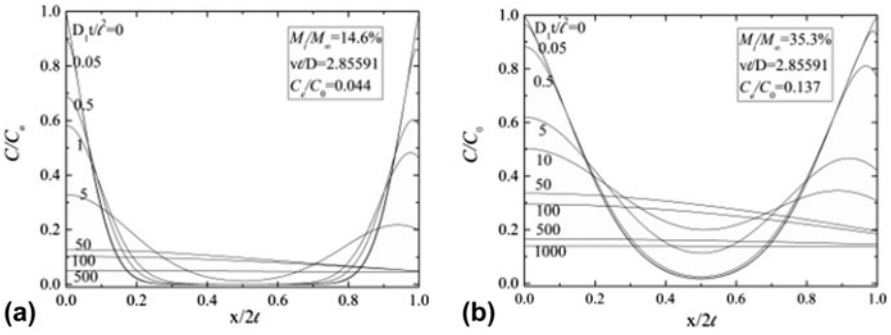


FIG. 3. Numerical results of the concentration distribution of the solvent in the PMMA slab of the one-side desorption at 25 °C for different times; (a) M_i/M_∞ = 14.6% and (b) M_i/M_∞ = 35.3%.

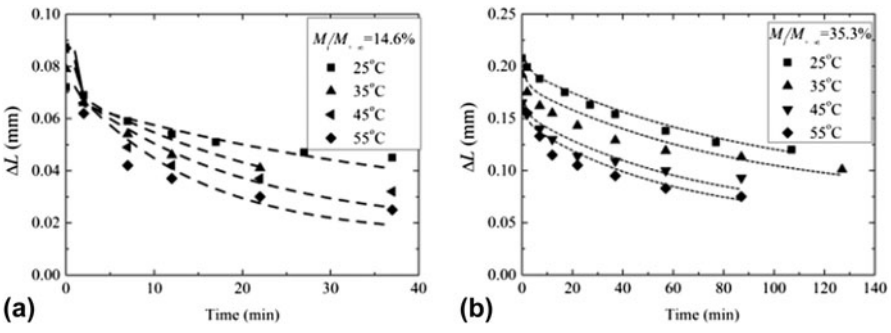


FIG. 4. Variation of the thickness change of the PMMA slabs with the desorption time at different temperatures; (a) M_i/M_∞ = 14.6% and (b) M_i/M_∞ = 35.3%.

https://doi.org/10.1557/jmr.2014.232 Published online by Cambridge University Press

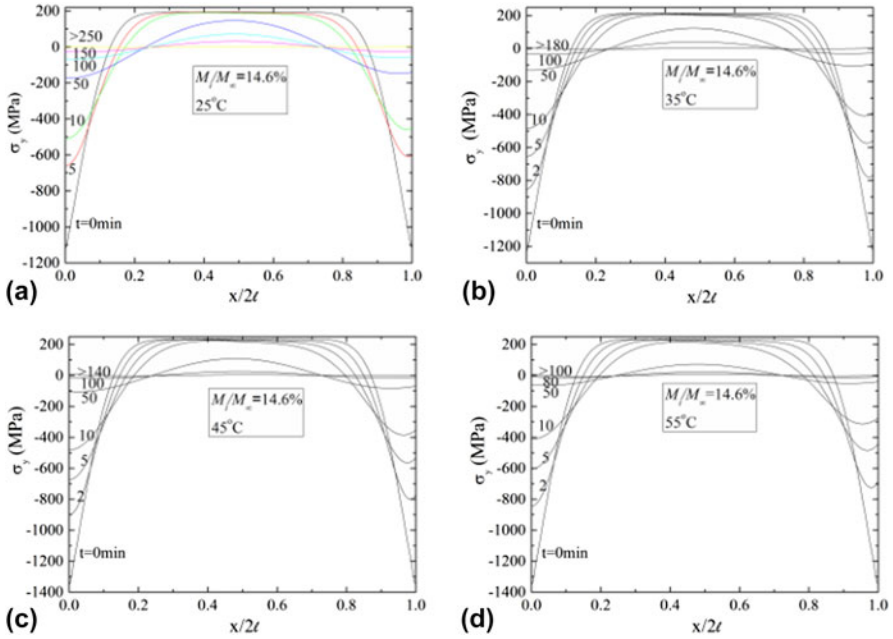


FIG. 5. Numerical results of the stress distribution in the PMMA slab with the one-side desorption and M_i/M_∞ = 14.6% for different desorption times at the desorption temperature; (a) 25 °C, (b) 35 °C, (c) 45 °C, and (d) 55 °C.

M_i/M_∞ = 14.6%, while it decreases with the increase of desorption temperature for the PMMA specimens of M_i/M_∞ = 35.5%. The mechanism for the dependence of the partial molal volume on the amount and distribution of methanol in the PMMA slabs is unclear. It might be related to the concentration gradient in the PMMA slabs which determines the migration rate of methanol.

Figure 5 shows the evolution of the stress distribution in the PMMA slabs during the desorption for M_i/M_∞ = 14.6% at different temperatures. The stress is calculated from Eq. (21), using the partial molal volume measured. The Young's modulus and Poisson's ratio of PMMA used are 7.4 GPa and 0.33, respectively.[25] At the surfaces of $x = 0$ and $x = 2\ell$, the PMMA slabs experience compressive stress, while in the central region, they experience tensile stress. The stress relaxes with the diffusion of methanol out of the PMMA slabs, and both the magnitudes of the tensile stress and the compressive stress decrease with the increase of the desorption time and approach the stress-free state. For a given time, the maximum magnitude of compressive stress shifts from the surface of $x = 0$ to inside the slab with increasing desorption time. The rate of the stress relaxation increases with the increase of the desorption temperature.

It is worth mentioning that the partial molal volume of methanol in PMMA and the Young's modulus of PMMA are generally functions of the concentration of methanol in PMMA, which depend on the concentration distribution. The partial molal volume is small for a small amount of methanol and increases significantly after the amount of methanol in PMMA reaches a critical value. The Young's modulus of PMMA decreases with the increase of the amount of methanol. The value of the partial molal volume obtained from Fig. 4 using Eq. (26) represents the average value of the partial molal volume of methanol in PMMA, and the effect of methanol on the Young's modulus of PMMA is assumed to be negligible in the stress calculation.

V. SUMMARY

Understanding the desorption behavior of solvents in polymers is of practical importance for the applications of polymers in a liquid environment, such as contact lens,[24] which experience water evaporation from the surface of the lens and their stiffness is related to desorption and the conformity with the eye ball. Considering the interaction between absorption and desorption of solvent in polymers, the stress evolution due to the desorption of solvent in a polymer slab was analyzed. The stress evolution is dependent on the concentration distribution of the solvent in the slab at the onset of the desorption and the desorption temperature. Using the diffusion-induced stress, an analytical relationship between the thickness change of a polymer slab and the partial molal volume of the solvent in the slab was obtained, which was used to determine the nominal partial molal volume of methanol in PMMA.

The desorption behavior of methanol in PMMA slabs was studied. The one-side desorption experiments were performed immediately following the absorption of methanol in the PMMA slabs in a methanol bath at 60 °C. From the residual amount of methanol in the PMMA slabs during the desorption, the diffusion

https://doi.org/10.1557/jmr.2014.232 Published online by Cambridge University Press

coefficient and the evaporation rate of methanol in the PMMA slabs as a function of temperature were determined, which followed the Arrhenius relation. The activation energies for the diffusion process and the evaporation rate of the solvent across the surface are 18.3, 42.6 and 8.6, 18.3 kJ/mol for the PMMA slabs with the values of M_i/M_∞ being 14.6% and 35.3%, respectively. Note that M_i and M_∞ are the initial amount of methanol during the desorption and the saturated amount of methanol during the absorption at 60 °C. The partial molal volumes are 78, 85, 94, and 94 cm^3/mol for the PMMA slabs with M_i/M_∞ being 14.6% at the desorption temperatures of 25, 35, 45, and 55 °C, respectively, and 90, 85, 73, and 70 cm^3/mol for the PMMA slabs with M_i/M_∞ being 35.5% at the desorption temperatures of 25, 35, 45, and 55 °C, respectively. The partial molal volume increases with the increase of the desorption temperature for the PMMA slabs of M_i/M_∞ = 14.6%, while it decreases with the increase of the desorption temperature for the PMMA slabs of M_i/M_∞ = 35.5%.

ACKNOWLEDGMENT

This work was financially supported by the Ministry of Science and Technology, Taiwan.

REFERENCES

1. A.T. Alfrey, E.F. Gurnee, and W.G. Lyod: Diffusion in glassy polymers. *J. Polym. Sci., C* **12**, 249 (1966).
2. S.P. Chen and J.A.D. Edin: Fickian diffusion of alkanes through glassy polymers: Effects of temperature, diffusant size, and polymer structure. *Polym. Eng. Sci.* **20**, 40 (1980).
3. J. Crank: *The Mathematics of Diffusion*, 2nd ed.; Oxford University Press: Oxford, UK, 1975.
4. N.L. Thomas and A.H. Windle: A theory of case II diffusion. *Polymer* **23**, 529 (1982).
5. A. Friedman and G. Rossi: Phenomenological continuum equations to describe case II diffusion in polymeric materials. *Macromolecules* **30**, 153 (1997).
6. C.Y. Hui and K.C. Wu: Case-II in polymers. I. Transient swelling. *J. Appl. Phys.* **61**, 5129 (1987).
7. C.Y. Hui and K.C. Wu: Case-II in polymers. II. Steady state front motion. *J. Appl. Phys.* **61**, 5137 (1987).
8. T.K. Kwei, T.T. Wang, and H.M. Zupko: Diffusion in glassy polymers. V. Combination of Fickian and case II mechanism. *Macromolecules* **5**, 645 (1972).
9. J.P. Harmon, S. Lee, and J.C.M. Li: Methanol transport in PMMA: The effect of mechanical deformation. *J. Polym. Sci., Part A: Polym. Chem.* **25**, 3215 (1987).
10. J.P. Harmon, S. Lee, and J.C.M. Li: Anisotropic methanol transport in PMMA after mechanical deformation. *Polymer* **29**, 1221 (1988).
11. I.J. Chiang, C.C. Chau, and S. Lee: The mass transport of ethyl acetate in syndiotactic polystyrene. *Polym. Eng. Sci.* **42**, 724 (2002).
12. S. Lee, T. Nguyen, E. Byrd, and J. Martin: Model of fatigue damage in strain rate-sensitive composite materials. *J. Mater. Res.* **18**, 2268 (2003).
13. C.S. Tsai, S. Lee, and T. Nguyen: Transport kinetics of methanol in hydroxyethyl methacrylate homopolymer and its copolymers. *J. Mater. Res.* **19**, 3359 (2004).
14. K.F. Chou, C.C. Han, and S. Lee: Transport kinetics of methanol in hydroxyethyl methacrylate homopolymer and its copolymers. *Polymer* **42**, 4989 (2001).
15. Y.H. Hwang, T. Matsui, T. Hanada, M. Shimoda, K. Matsumoto, and Y. Osajima: Desorption behavior of sorbed flavor compounds from packaging films with ethanol solution. *J. Agric. Food Chem.* **48**, 4310 (2000).
16. B. Muir, H.B. Duffy, and M.C. Moran: Optimization of solvent desorption conditions for chemical warfare agent and simulant compounds from Porapak Q™ using experimental design: I. Methyl salicylate and di(propylene glycol) monomethyl ether. *J. Chromatogr. A* **1038**, 183 (2004).
17. S.C. Anand, J.F. Kennedy, M. Miraftab, and S. Rajendran: *Medical Textiles and Biomaterials for Healthcare* (CRC Press, Boca Raton, FL, 2006).
18. Y. He and X. Fan: In-situ characterization of moisture absorption and desorption in a thin BT core substrate. In *Proc. of 2007 IEEE 57th Electronic Components and Technology Conference, 29 May–1 June*, Sparks, Nevada, 1376 (2007).
19. H. Yang, Q.T. Nguyen, Z. Ping, Y. Long, and Y. Hirata: Desorption and pervaporation properties of zeolite-filled poly(dimethylsiloxane) membranes. *Mater. Res. Innovations* **5**, 101 (2001).
20. A-C. Saby-Dubreuil, B. Guerrier, C. Allain, and D. Johannsmann: Glass transition induced by solvent desorption for statistical MMA/nBMA copolymers - Influence of copolymer composition. *Polymer* **42**, 1383 (2001).
21. C.J. Gommes, F. Noville, and J-P. Pirard: Characterization of gels via solvent desorption measurements. *Adsorption* **13**, 533 (2007).
22. F.Q. Yang: Interaction between diffusion and chemical stresses. *Mater. Sci. Eng., A* **409**, 153 (2005).
23. F.Q. Yang: Diffusion-induced stress in inhomogeneous materials: Concentration-dependent elastic modulus. *Sci. China: Phys., Mech. Astron.* **55**, 955 (2012).
24. G. Gates, J.P. Harmon, J. Ors, and P. Benz: 2,3-Dihydroxypropyl methacrylate and 2-hydroxyethyl methacrylate hydrogels: Gel structure and transport properties. *Polymer* **44**, 215 (2003).
25. C.K. Liu, S. Lee, L.P. Sung, and T. Nguyen: Load-displacement relations for nanoindentation of viscoelastic materials. *J. Appl. Phys.* **100**, 033503 (2005).

https://doi.org/10.1557/jmr.2014.232 Published online by Cambridge University Press